GBS|CIDP Foundation International - Benson Clinical Research Fellow

Biomarkers in the diagnosis and follow-up of CIDP: Final Report.

OVERAL AIM:

To develop the "Inflammatory Neuropathy" clinic in which a systematic and prospective multiparametric collection of clinical data, biomaterials and digital biomechanical parameters (through wearable devices) will be use to discover and validate novel disease-monitoring strategies informed by biological biomarkers and biomechanical data, and a diverse range of validated inflammatory neuropathy scores and scales that would serve as validated anchors to assign clinical relevance to the novel monitoring parameters.

SUBPROJECT 1: NEW CIDP-SPECIFIC AUTOANTIBODIES

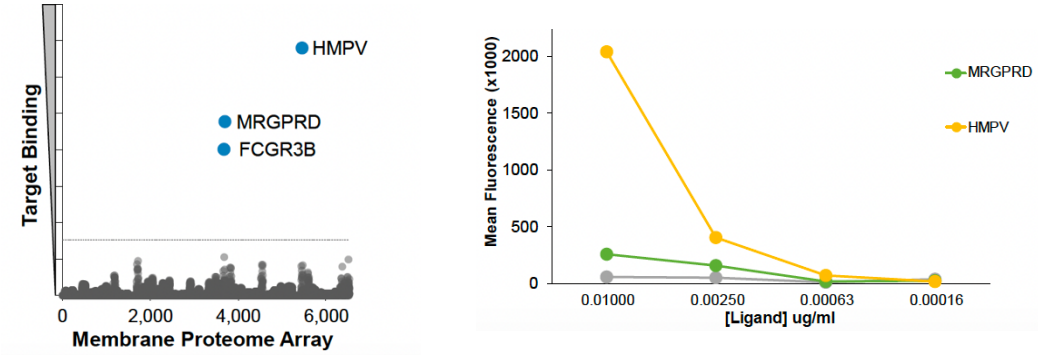
Objective: **To investigate new CIDP-specific autoantibodies using a novel autoantibody-discovery strategy of protein arrays that display in their native conformation thousands of secreted and membrane-bound proteins of the human proteome, using human cell lines**.

- In a previous project we were able to validate the ***Retrogenix Cell Microarray*** with known antigens and demonstrated that patients' derived anti-NF155 and anti-CNTN1 IgG are detected by this novel cell microarray. Then, sera from 4 patients with typical CIDP and 4 patients with CIDP with antibodies against neural structures (DRG neurons, neuroblastoma-derived human motor neurons and macaque sciatic nerve) were screened for the presence of IgG autoantibodies with the Retrogenix cell microarray technology. Six relevant reactivities were found: Ephrin type-A receptor 7 (EPHA7), potassium-transporting ATPase alpha chain 1 and subunit beta (ATP4A/4B), leukemia inhibitor factor (LIF) and interferon lambda 1,2 and 3 (IFNL1, IFNL2 and IFNL3). Candidate antigens were validated by cell-based assays (CBA), ELISA and/or tissue immunohistochemistry, and analyzed in a cohort of CIDP (n=96) and control (n=100) samples. Anti-ATP4A/4B and anti-EPHA7 antibodies were detected in patients and controls and considered unrelated to CIDP. Both anti-LIF and anti-IFNL antibodies were found in the same 2 patients and were not detected in any control. Both patients showed the same staining pattern against myelinating fibers of peripheral nerve tissue and of myelinating neuron-Schwann cell cocultures. Clinically relevant correlations could not be established for anti-LIF and anti-IFNL3 antibodies. Our work demonstrated the utility of human cell microarray technology to detect known and discover unknown autoantibodies in human serum samples. Despite potential CIDP-associated autoantibodies (anti-LIF and anti-IFNL3) being identified, their clinical and pathogenic relevance needs to be elucidated in bigger cohorts. These results were recently reported (*Caballero-Ávila M, Lleixà C, Pascual-Goñi E… Querol L. Membrane Proteome-Wide Screening of Autoantibodies in CIDP Using Human Cell Microarray Technology. Neurol Neuroimmunol Neuroinflamm. 2024 May;11(3):e200216. doi: 10.1212/NXI.0000000000200216. Epub 2024 Mar 14.)*

- To further investigate novel antibodies against membrane proteins in CIDP, we tested 3 serum pools, each comprising samples from nine seronegative CIDP patients—2 for **IgG**

and the other for **IgM**—using the ***Integral Molecular Membrane Proteome Array (MPA).*** The MPA is a platform for profiling the specificity of antibodies and other ligands that target human membrane proteins. The MPA can be used to determine antibody target specificity and deconvolute orphan antibody/ligand targets. The platform uses flow cytometry to directly detect antibody binding to membrane proteins expressed in unfixed cells. Consequently, all target proteins have native conformations and appropriate post-translational modifications. Our samples were tested for reactivity against a library of over 6,000 human membrane proteins, including 94% of all single-pass, multi-pass, and GPI-anchored proteins, including GPCRs, ion channels, and transporters. Identified targets were validated in secondary screens to confirm reactivity.

Figure 1. MPA screen and validation results for newly identified ligand targets (IgG). Each ligand was tested for binding by flow cytometry against the MPA at the previously determined optimal concentration. Binding interactions confirmed in downstream validation studies are displayed in blue and any proteins that did not pass validation were removed. Serial ligand dilutions were incubated with newly identified targets and binding was measured by flow cytometry. A target was validated if it demonstrated binding signal ≥2-fold above background at the two highest concentrations tested.



- The **MPA** failed to detect anti-NF155 IgG and anti-MAG IgM antibodies. **IgG** screening using the MPA identified three significant reactivities: Mas-related G-protein coupled receptor member D (MRGPRD), Low affinity immunoglobulin gamma Fc region receptor III-B (FCGR3B), and Human metapneumovirus (HMPV). Of these, HMPV and MRGPRD passed all validation criteria and were considered true binding interactions by MPA technology, but only MRGPRD, a G protein-coupled receptor expressed in the peripheral nervous system (PNS), emerged as a relevant candidate antigen in CIDP. Among the candidate targets identified in the first step but that did not fulfill all validation criteria were protein-coupled receptor 157 (GPR157), an orphan G protein-coupled receptor s highly expressed in the CNS and ransient Receptor Potential Melastatin 3 (TRPM3), a calcium-permeable ion channel that belongs to the Transient Receptor Potential channel superfamily and is strongly expressed in the PNS. **IgM** screening identified two significant reactivities that passed all validation criteria and were considered true binding interactions: Low-Density Lipoprotein Receptor-Related Protein 8 (LRP8) a member of the LDL receptor family expressed in the central and peripheral nervous system, involved in both lipid metabolism and neuronal signaling and G Protein-Coupled Receptor 101 (GPR101), expressed in the brain and pituitary, implicated in neuroendocrine regulation.

- **Validation studies** were conducted in our laboratory using cell-based assay (CBA) for each antigen. In **CBA**, mammalian expression vectors encoding human MRGPRD,

GPR157, TRPM3, LRP8 and GPR101 were transfected into HEK293 cells using Lipofectamine 2000 (Invitrogen, CA). Cells were then fixed with 4% paraformaldehyde and blocked with goat serum 5%. ICC experiments were performed using patients' sera and appropriate primary and secondary antibodies (Table 1). **ELISA** was performed using maxisorb 96-well ELISA plates (Thermo Fisher Scientific, NUNC, Denmark) coated overnight with 5ug/ml MRGPRD recombinant human protein. Wells were blocked with 5% non-fat milk in PBS 0.1% Tween20 for 1 hour, incubated with diluted sera for 1 hour, and then incubated with peroxidase conjugated rabbit anti-human IgG secondary antibodies for 1 hour at room temperature. ELISA was developed with tetramethylbenzidine solution (BioLegend, CA), and the reaction was stopped with 25% sulfuric acid. Optical density (OD) was measured at 450 nm in a Multiscan ELISA reader. Samples were considered positive by ELISA when they had a ΔOD higher than the average healthy control ΔOD plus 2 standard deviations.

Table 1. List of candidate antigens evaluated by CBA and ELISA

Method	Antigen	c-DNA clone/ RH Protein	Sera dilution	Primary antibody	Secondary antibody	Result
CBA	MRGPRD	NM_198923.2; OHu29581 (Genscript)	1:100	MRGPRD (Sigma) 1:200	GAH IgG 594, GAR 488 1:1000	Negative
	GPR157	NM_024980.5; OHu04306 (Genscript)	1:100	Anti-DYK (Origene) 1:500	GAH IgG 594, GAM 488 1:500	Negative
	TRPM3	NM_020952; RC218008 (Origene)	1:50	Anti-cmyc (Merck) 1:200	GAH IgG 594, GAM 488 1:500	Negative
	LRP8	NM_004631.5; OHu23113 (Genscript)	1:50	Anti-DYK (Origene) 1:500	GAH IgM 594, GAM 488 1:500	Negative
	GPR101	NM_054021; RC210183 (Origene)	1:50	Anti-cmyc (Merck) 1:200	GAH IgM 594, GAM 488 1:500	Negative
ELISA	MRGPRD	CSB-CF844729HU (Cusabio)	1:100	-	RAH IgG HRP (Agilent) 1:3000	Negative

- We were unable to confirm specific IgG/IgM reactivity against the candidate antigens in any of the CIDP serum samples included in the initial pools.

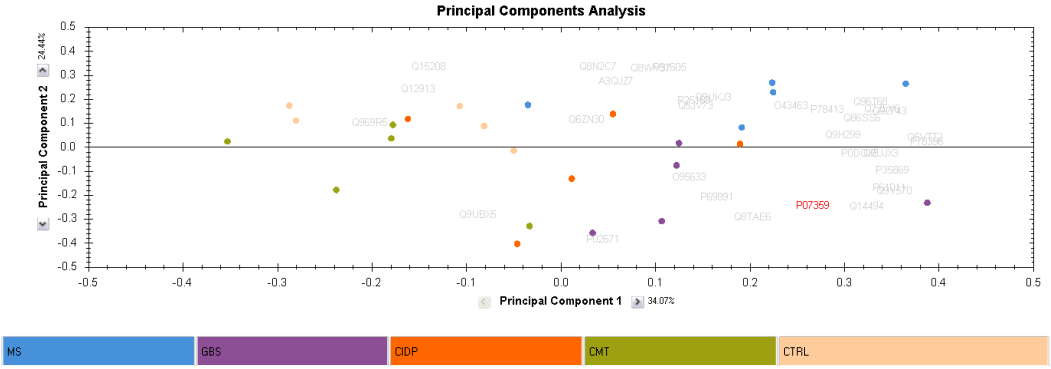
SUBPROJECT 2: CIDP ACTIVITY BIOMARKERS

Objective: **To investigate novel biological markers informing on nerve damage (myelin and axonal damage biomarkers) and disease activity (inflammation biomarkers) with clinical utility in the diagnosis and follow-up of CIDP**

- Myelin biomarkers: We performed a myelin-damage biomarkers discovery in CSF of patients with demyelinating disorders The following samples were included in this discovery experiments: CSF samples from 5 patients with the AIDP GBS variant, 5 patients with aggressive CIDP, 5 patients with severe multiple sclerosis (disease control: autoimmune-demyelinating disease of the CNS), 5 patients with demyelinating neuropathies of genetic cause (Charcot-Marie-Tooth, disease control: non-

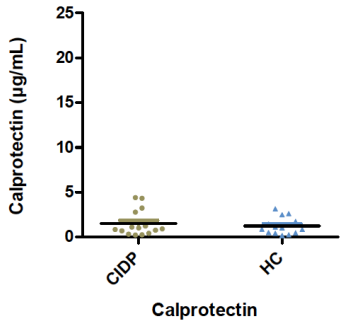
inflammatory demyelinating disease) and 5 controls. These 25 samples were analyzed by mass spectrometry and a specific software designed to classify and differentiate the protein profiles of the different groups, with special emphasis on myelin-specific proteins that are shared among demyelinating diseases. This analysis demonstrated 9 proteins differentially expressed in CIDP vs controls; 23 proteins differentially expressed in GBS/CIDP/GBS/CMT vs controls; 38 proteins differentially expressed in GBS/CIDP/MS (demyelinating diseases) vs controls; 25 proteins differentially expressed in CIDP/GBS/CMT (peripheral nerve diseases) vs controls. However, none of the differentially expressed proteins were considered relevant according to their function, tissue expression or relevance to disease.

Figure 2. Analysis of CSF protein profiles in MS, GBS, CIDP, CMT and controls.



- Inflammation biomarkers: Calprotectin is a protein mainly involved in inflammatory processes and correlates with disease activity in systemic autoimmune disorders. Recently, it was proposed as a potential biomarker in CIDP to monitor disease activity (F Stascheit 2021). In an exploratory study we tested calprotectin levels in sera from patients with CIDP (n=15) and healthy controls (n=15). Calprotectin was test by a chemiluminescence assay. No significant differences were found between both groups (1.5±1.4µg/mL vs 1.2±0.9µg/mL; p=1). Thus, we were not able to confirm that calprotectin is a potential disease-activity biomarker in CIDP patients.

Figure 3. Calprotectin serum levels measured in CIDP and HC.



- Axonal damage biomarkers: serum neurofilament light chain (sNfL) were tested using Single Molecule Array (SiMoA) technology, in serum samples collected during the monitoring visit of this study protocol.

Figure 4 shows the analysis of sNfL levels and Z-scores across the different disease groups and their relationship with disease activity. These results were presented at the Peripheral Nerve Society (PNS) Annual Meeting, held in Maastricht, the Netherlands, in June 2026.

SANT PAU Campus Salut Barcelona

Hospital de la Santa Creu i Sant Pau

Serum neurofilament light chain for monitoring disease activity in chronic inflammatory neuropathies: a real-world study

Elba Pascual-Goñi[1,2], Roger Collet-Vidiella[1], Clara Tejada-Illa[1], Paula Llarch1, Manuel Cabezas[1], Lorena Martín-Aguilar[1], Marta Caballero-Ávila[1], Tania Mederer[1], Gemma Riesco-Navarro[1], Cinta Lleixà[1], Juan Castilla Silgado[1,2], Luis Querol[1,2].

1.Neuromuscular Diseases Unit, Department of Neurology, Hospital de la Santa Creu i Sant Pau, Universitat Autònoma de Barcelona, Spain

2.Centro para la Investigación Biomédica en Red en Enfermedades Raras (CIBERER), Madrid, Spain.

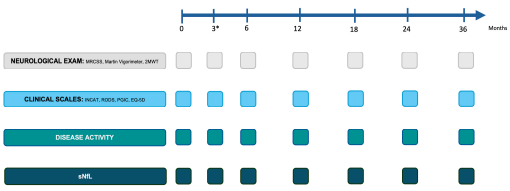
Background and Methods

Reliable biomarkers reflecting disease activity and treatment response in chronic inflammatory neuropathies (CIN) are still lacking. Serum neurofilament light chain (sNfL) has emerged as a promising marker of axonal injury in these disorders. We aimed to evaluate the role of sNfL as a biomarker of disease activity in patients with IN in a real-world clinical setting.

We conducted an observational study including 94 patients with chronic IN followed at our neuromuscular unit for up to 36 months. Patients were monitored every 6 months according to the protocol detailed in Figure 1.

Disease activity in Chronic Inflammatory Demyelinating Polyneuropathy (CIDP) and Chronic Ataxic Neuropathy with Ophthalmoplegia, IgM M Protein, Agglutinins and Disialosyl Antibodies (CANOMAD) was classified as active or non-active based on the treating physician's assessment. SNfL levels were measured at each visit using Simoa, and Z-scores sNfL (Z-sNfL) were calculated. The proportion of patients with Z-sNfL values >1.5 was analyzed, and its association with disease activity was assessed, as this threshold has been associated in other neurological disorders, including multiple sclerosis, with an increased risk of disease activity and worse clinical outcomes. Longitudinal associations between Z-sNfL levels and disease activity were assessed in the CIDP subgroup using linear mixed-effects models accounting for repeated longitudinal measurements within each patient. Disease activity and follow-up time from baseline were included as fixed effects.

Figure 1. Study protocol.



* Unstable patients

Results

The cohort included 44 CIDP, 13 Anti-Myelin-Associated Glycoprotein (MAG) neuropathy, 9 Multifocal Motor Neuropathy (MMN), 8 autoimmune nodopathies (AN) including 6 anti-NF155+, 1 anti-Pan-NF+ and 1 anti-Caspr1+, 6 CANOMAD, 2 Chronic Immune Sensory Polyradiculopathy (CISP), and 12 patients with other CIN including 4 cases of neuropathies associated with IgM M Protein and 8 patients with polyradiculopathy who did not fulfill the diagnostic criteria for CIDP.

Baseline sNfL levels and Z-sNfL for each disease subgroup are shown in Figure 2. Baseline Z-sNfL values were above 1.5 in 23% CIDP, 15% anti-MAG neuropathy, 33% MMN, 38% AN, 67% CANOMAD, 50% CISP, and 8% other CIN patients.

Post-treatment Z-sNfL data were available for three patients with active CANOMAD, each receiving a different treatment regimen (daratumumab, rituximab plus IVIG, and IVIG monotherapy). All showed a decrease in Z-sNfL to <1.5, as shown in Figure 3C accompanied by substantial clinical improvement.

In the CIDP subgroup, linear mixed-effects models accounting for repeated measurements demonstrated that disease activity was independently associated with higher longitudinal Z-sNfL levels (= 0.44, 95% CI 0.09–0.79, p = 0.014). Z-sNfL levels also showed a mild decrease over time during follow-up (= -0.014/month, 95% CI -0.026 to -0.001, p = 0.028).

Figure 2. Baseline sNfL levels, Z-sNfL values, and the percentage of patients with baseline Z-sNfL >1.5 in each disease subgroup.

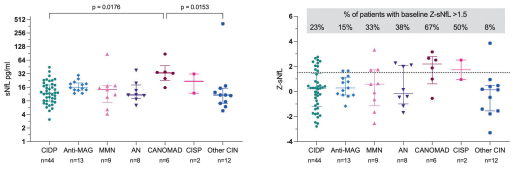


Figure 3A and 3B show the Z-sNfL values in patients with active and non-active CIDP and CANOMAD, respectively. In the CIDP subgroup, 43% showed disease activity during follow-up. Median Z-sNfL levels (1.34 vs 0.28; p=0.27) and the proportion of patients with Z-sNfL >1.5 (42% vs 16%; p=0.09) tended to be higher in active patients. In the CANOMAD subgroup, 67% were active at baseline, all of whom had Z-sNfL >1.5 compared with none of the on-active (p=0.067), with higher median Z-sNfL (2.58 vs 0.76; p=0.13).

Figure 3. Z-sNfL values in active and non-active CIDP and CANOMAD, and pre- and post-treatment z-sNfL values in CANOMAD.

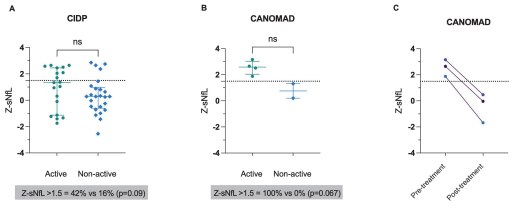


Table 1. Baseline characteristics of the patient cohort included in the study.

	CIDP	Anti-MAG	MMN	Autoimmune nodopathies	CANOMAD	CISP	Other CIN
Sujects (n)	44	13	9	8	6	2	12
Age years, median (IQR)	59 (50-68)	72 (61-77)	59 (52-62)	61 (37-71)	69 (60-81)	53 (52-53)	64 (56-68)
Baseline sNfL (pg/ml), median (IQR)	11,9 (7,9-18,1)	15,7 (13,9-20,0)	14,3 (7,4-17,3)	10,8 (9,1-18,0)	33,4 (22,7-48,1)	21,8 (11,9-31,7)	10,8 (7,0-15,3)
Baseline Z-sNfL median (IQR)	0,27 (-1,18-1,44)	0,28 (-0,28-1,14)	0,58 (-1,14-1,73)	-0,14 (-1,00-2,07)	2,20 (0,61-2,78)	1,73 (0,95-2,51)	0,13 (-1,55-0,47)
Baseline Z-sNfL > 1.5, %	23	15	33	38	67	50	8

Conclusions

In a real-world setting, sNfL appears to be a useful biomarker of disease activity in selected patients with chronic inflammatory neuropathies, providing complementary information for disease monitoring and treatment response assessment. In particular, longitudinal changes in sNfL may better reflect ongoing disease activity and clinical evolution. Larger prospective studies are needed to validate these findings and determine the broader applicability of sNfL in routine clinical practice.

Grant support

Instituto Carlos III (Spain), Fondo Investigaciones Sanitarias (FIS) PI22/00387 and Benson fellow GBS-CIDP foundation.

Acknowledgments

We thank Professor Jens Kuhle for providing the Z-sNfL data derived from the sNfL measurements of our patients.

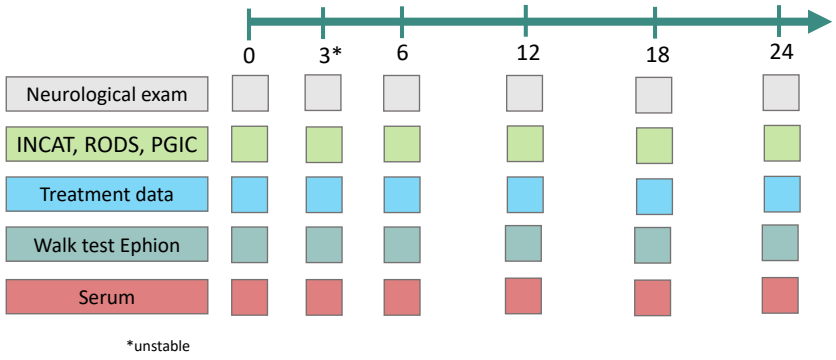
Contact: epascualg@santpau.cat

- Longitudinal analyses evaluating the association between sNfL levels and disease activity, neurological examination (MRC, vigorimerter), clinical assessment scales (INCAT, RODS, 2MWT) are currently underway.

SUBPROJECT 3: WEARABLE BIOMECHANICAL TECHNOLOGY

Objective: **To assess the clinical utility of a wearable system of intensive biomechanical monitoring that includes surface electromyography, gait assessment with oscillometers and foot pads, and heart rate assessment to monitor clinical status of CIDP patients.**

Figure 5. Study protocol: Patients were monitored every six months for two years. Unstable patients were also be monitored at the time of the relapse and 3 months after treatment adjustment. We will correlate data from the wearable system with the neurological examination (MRC, MIRCAR-SARA Ataxia scale, Martin Vigorimeter), scales (INCAT), patient-reported outcome measures (IRODS) and biological biomarker of axonal damage (sNfL).



- A total of 100 patients with inflammatory neuropathies recruited, including 50 CIDP patients and 50 with other inflammatory neuropathies (9 MMN, 22 MGUS-P, 6 CANDA/CANOMAD, 8 autoimmune nodopathies (AN), and 5 GBS). Also, 13 patients with CMT were included as disease controls. By the end of June 2025, 62 patients completed the 2-year follow-up, and 32 completed at least 1 year of follow-up. All patients performed the following timed walking tests wearing the Ephion Health System: 2MWT, timed 25-feet-walking test, timed up and go test. Also, Romberg and Tandem tests were recorded.

- We used the Ephion Health System, a wearable system developed by Ephion Health that integrates multi-parameter sensors from various sources including 6 inertial sensors (Movesense), tights with EMG surface sensors (Myontec), insoles with inertial and plantar pressure sensors (Moticon) and a pectoral heart rate monitor (Movesense). All sensors are synchronized using the Ephion Mobility software on a Smartphone. Although the full protocol included pants with integrated surface EMGs, for the purpose of this study, these data were not analyzed

- **We first performed a study to test the ability of a set of digital biomechanical features, consisting of multiple spatiotemporal features, biomechanical angles, and plantar pressure parameters, to monitor the clinical status of patients with inflammatory neurpathies**. To achieve this goal, three objectives were developed. First, we

investigated whether DBF could detect differences from healthy controls in two frequent gait phenotypes that appear in patients with PNs: gait ataxia and steppage gait. Second, we analyzed whether DBF was correlated with impairment and disability clinical scales. Third, we tested the ability of DBF to capture clinically significant changes over time. We included 37 CIDP, 3 CANOMAD, 21 IgM-MGUSP, 7 AN, 11 CMT patients, and 50 healthy controls. Patients were classified by the evaluating neurologist according to their gait pattern into three gait groups (ataxia gait, steppage or normal gait). Additionally, the severity of ataxia and steppage (mild, moderate, or severe) was classified according to criteria specified in table 2.

Table 2. Gait pattern classification in ataxia or steppage and according to de severity.

	Ataxia MICARS-SARA item1 (walking capacities)	**Steppage MRC-SS Ankle Dorsiflexion item (Right + Left)**
Severe	Value ≥ 5	Value ≤ 4
Moderate	Value 3-4	Value 5-6
Mild	Value 1-2	Value 7-8
Normal	Value 0	Value ≥ 9

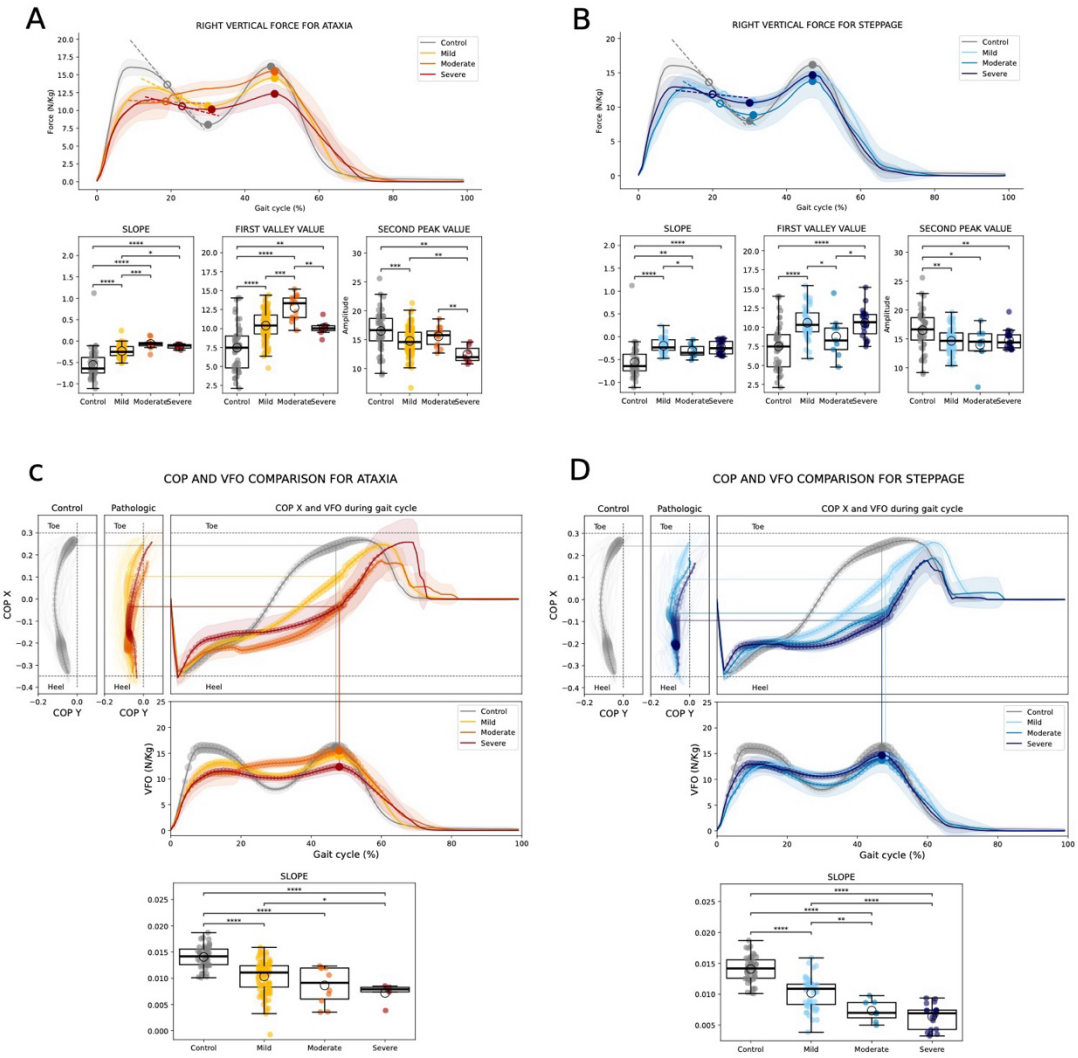
- Data collected from the entire 2MWT was segmented into gait cycles, which start and end when the same foot contacts the ground. A step detection algorithm using angular velocity on the sagittal plane and plantar pressure values was used to identify gait cycles in each sensor. Each gait cycle was normalized to 100 samples, representing 0 to 100% of the gait cycle, and averaged to obtain the mean pattern. This normalization facilitates the comparison of tests at different velocities. Various characteristics of the curves were then calculated from this mean cycle. A total of six gait profiles (variables) were analyzed, including the kinematics of the hip joint, knee joint, ankle joint, and foot segment, as well as the vertical force and center of pressure evolution. Joint angles were calculated using relative segments as references, whereas the foot segment used the global reference frame.

- **First, we analyzed the sensor's ability to detect changes in ataxia and steppage gait severity and found significant differences in spatiotemporal and angular variables of the gait cycle.** The spatiotemporal features velocity, stride duration and length, cadence, and double support time were analyzed for both groups of patients (Fig. 2). In patients with ataxia, there were significant overall differences between severity groups for each parameter. Velocity, stride length, and cadence all showed significant decreases when ataxia severity increased, while stride duration and double support time increased correspondingly. A similar pattern was observed in the steppage cohort with significant differences in the overall and with similar trends as those observed in the ataxia group.

  Vertical force (VF) was analyzed throughout a gait cycle (Figure 6 A, B). For visual and analytical purposes, 3 features of the cycle were highlighted: the slope of the curve, the value in the valley, and the value of the second peak. In the ataxia group the curves presented significantly flatter slopes compared to the control and smaller second peak. For the steppage group, differences in slopes were also significantly flatter in comparison to the control group with higher valley values and a reduced second peak. The center of pressure (COP) of the VF (Figure 6 C, D) over the insole during a gait cycle is displayed in Figure 7. Differences in slope and toe-off time were observed for both ataxia and steppage groups. A reduction of this feature was detected across the

different severity groups (except for the moderate and severe groups in ataxia). In normal controls, the weight is distributed mainly between the heel, at the beginning of the cycle, and the toe, at the end of the cycle. In ataxia patients, the weight was distributed on the heel and along the foot during the gait cycle, and there was almost no support of the weight with the toe. Similar findings were observed for steppage patients, although differences across the severity groups were clearer. In patients with severe steppage, support almost exclusively happened on the heel. In addition, the value of the slope decreased significantly in the different severity groups.

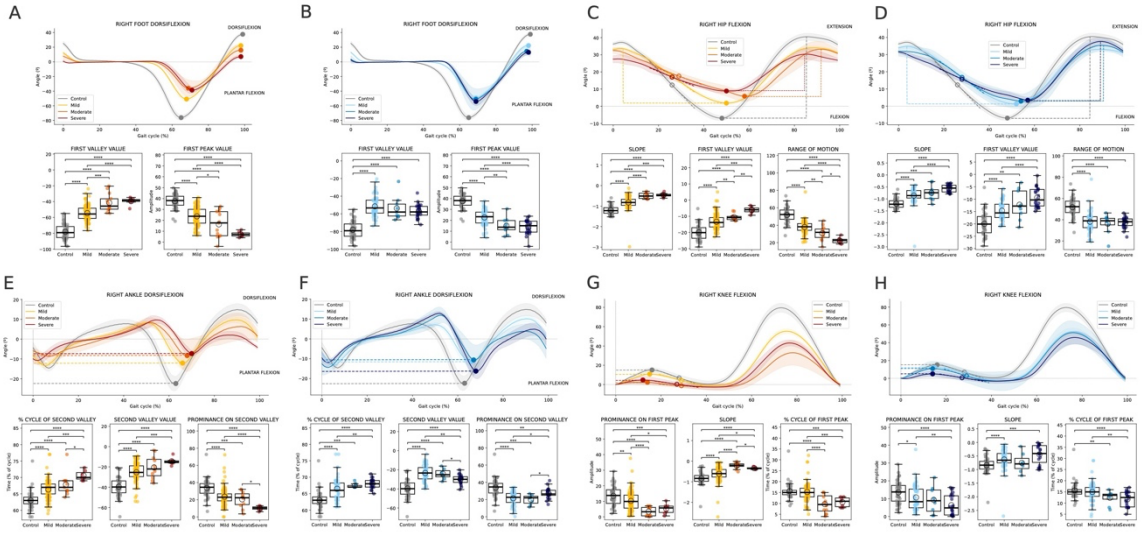
Figure 6. Vertical force (VF) and center of pressure (COP) during one gait cycle in ataxia (A) and steppage (B) groups. The pairwaise comparisons of the four groups uncorrected differences between groups patients and controls are represented as follows: **** -> p uncorrected<0.0001, *** -> p uncorrected<0.001, ** -> p uncorrected<0.01, * -> p uncorrected<0.05.



Significant global differences were found in the angular variables (Figure 7) in both ataxia and steppage groups. Foot angle flexion (Figure 7 A, B) analysis revealed that patients with ataxia presented a significant decrease in negative foot angle flexion across the different severity groups compared with the control group during the double support phase, represented by the valley value. The same occurred during the final

phase of the cycle, which corresponded to the value in the second peak, in which we observed a significant decrease in positive foot angle flexion in the different severity groups compared with the control group. Compared to the control group, the angle of flexion of the negative foot angle decreased during the double support phase, and the angle of flexion of the positive foot angle also decreased during the final acceleration phase in the group of steppage patients. However, the differences between the severity groups were smaller than those between the ataxia groups. The hip angle flexion (Figure 7 C, D) analysis revealed a decreased slope feature and a significantly lower negative hip angle across the different severity groups of ataxia patients. The range of motion feature was also significantly lower in the different severity groups. For the steppage group, significant differences were observed in the value of the slope for the three severity groups compared with the control group. The values at the valley and the range of motion significantly changed only when patients and controls were compared but not across the three severity groups. The ankle angle flexion (Figure 7 E, F) analysis revealed a delay in the appearance of the valley in patients with ataxia. A decrease was also observed in the negative value of the valley feature across the different severity groups compared with the control group. For this variable, the proportion of the cycle in the second valley significantly decreased across the different severity groups. The opposite occurred for the prominence feature, which increased significantly across the severity groups. For steppage patients, the same findings were observed: a delay in the appearance of the valley, a decrease in the negative value of the valley and in the % cycle of the second valley, and an increase in the prominence feature. The differences across severity groups were less prominent than those in the ataxia group. In the knee angle flexion variable (Figure 7 G, H), we observed a flattening of the entire first phase of the gait cycle observed in patients with ataxia, with a significant decreased in the slope (close to 0 across the different severity groups). The prominence and proportion of first peak features significantly decreased (except for those in the severe group) across the different severity groups. For the steppage group of patients, the same trends were observed: a decrease in the negative slope and a decrease in the prominence and proportion of first peak features. However, significant differences were obtained only when patients and controls were compared and not across all severity groups.

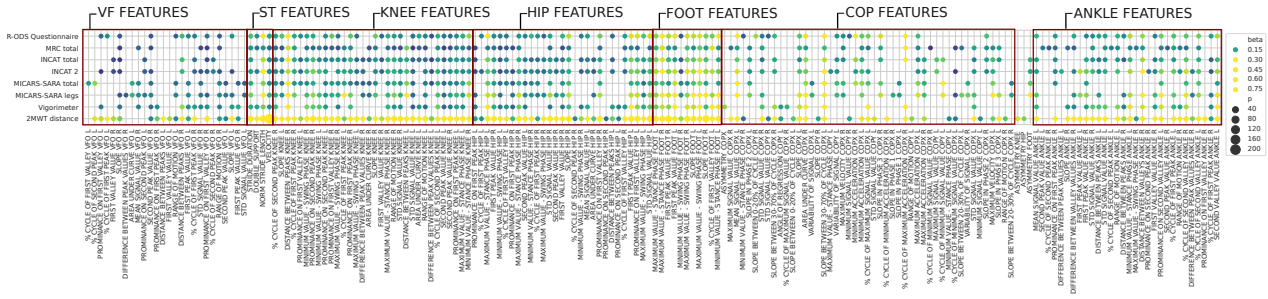
Figure 7. Foot, hip, ankle, and knee angle flexion variables during one gait cycle in ataxia (A,C,E,G) and steppage patients (B,D,F,H). The Kruskal–Wallis test was performed, followed by post hoc comparisons via Tukey's HSD test. The pairwaise comparisons of the four groups uncorrected differences between groups of patients and controls are represented as follows: **** -> p uncorrected<0.0001, *** -> p uncorrected<0.001, ** -> p uncorrected<0.01, * -> p uncorrected<0.05.



- **Second, we found correlations between biomechanical features and clinical scales and with the specific gait phenotype they associated with.** Linear mixed-effects (LME) models analysis revealed 219 biomechanical features associated with ataxia, steppage or both gait patterns. Among these features, 131 features were associated with ataxia, 94 with steppage, and 133 with both gait patterns. Among these features, 24 were associated only with ataxia, and 10 were associated only with steppage. Interestingly, while the features associated with only gait ataxia were related mainly to plantar pressure and hip features, those correlated with steppage were related mainly to COP features. Significant differences in COP features were observed among steppage patients and across the severity groups. Biomechanical features related to the foot, knee, ankle, and spatiotemporal variables correlated with both gait ataxia and steppage gait. To analyze which biomechanical features correlated with the different clinical scales the full cohort of patients was included, and the LME test was used. A total of 219 features were extracted, and 182 of them correlated significantly with any of the impairment (MRCss, MICARS-SARA, and vigorimeter) or disability (INCAT and iRODS) clinical scales and the 2MWT. Four spatiotemporal features, 11 foot features, 10 hip features, and 17 knee features were strongly correlated with all the clinical scales and the 2MWT. Thirty-seven (17%) features did not correlate with any clinical scale. Other features related to the VF, COP, hip and ankle correlated with some but not all the scales, and 19 (8.7%) of them correlated with only one clinical scale or 2MWT. Focusing on the scales, iRODS correlated with 112 features (51.1%), MRCss with 100 features (45.7%), INCAT with 115 features (52.5%), MICARS with 96 features (43.8%), vigorimeter with 95 features (43.4%) and 2MWT with 147 features (67.1%) related to some of the VF, COP, knee, hip, and ankle features (Figure 8).

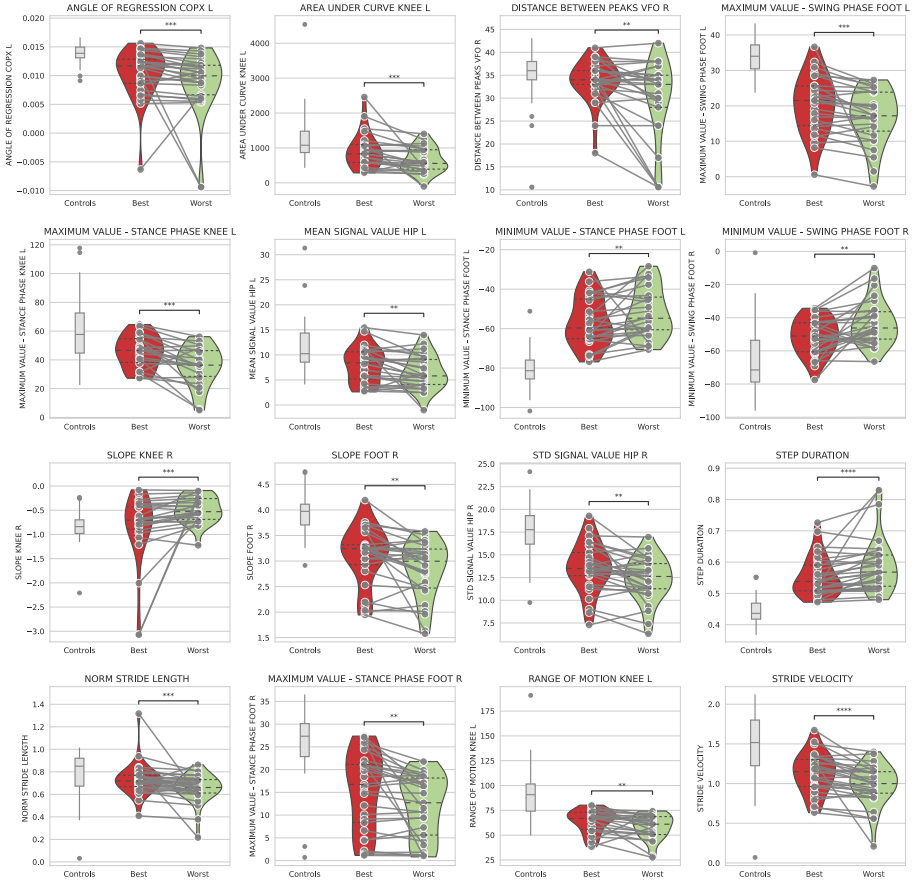
Figure 8. Correlation of clinical scales with biomechanical features. Color intensity and size of the bubbles represent the correlation level of the features with their gait pattern. Non-normalized and normalized scales are represented using the logarithm of the total score. Multiple comparisons were performed and a significance level of FDR-corrected p-value <0.05 was established to select features that correlated with their gait pattern. Only plotted significant features. VF: Vertical force; ST: spatiotemporal; COP: Center of pressure; MRCss: Medical Research Council sum score, INCAT: Inflammatory Neuropathy Cause and Treatment, iRODS: Inflammatory Rasch-built Overall Disability

Scale, MICARS-SARA: Modified Internacional Cooperative Ataxia Rating Scale and Scale for the Assessment and Rating of Ataxia, 2MWT: 2-minute walking test.



- **Finally, we demonstrated that this technology is able to capture clinically significant changes in gait features over time.** Patients selected for these analyses included those who presented clinically meaningful worsening or improvement, defined as (1) a 2-point or greater change in the MRC score and/or (2) a 4-point change on the iRODS scale, which are conventional definitions for minimal clinically important differences in inflammatory neuropathies. We detected 41 CIDP patients (119 tests), 20 IgM-MGUSP (54 tests), and 11 CMT (16 tests) that fulfilled these criteria and compared their results with those of a longitudinal assessment of 50 healthy controls. When the best and worst clinical assessments in patients who showed a significant change in the MRCss scale were selected, significant differences were observed in 16 biomechanical features (Figure 9), mainly those related to foot biomechanics. Additionally, differences were observed for COP variables and stride length features. Using the same statistical test but with a cohort of patients who presented a change of at least 4 points on the iRODS scale, we did not detect significant changes in any biomechanical feature, probably because the iRODS, a subjective scale, may fluctuate in the absence of objective change. When all available longitudinal assessments with LME analysis were used in a cohort of patients who presented a clinically relevant change in the MRCss at any time point, the DBF system was able to identify 28 different biomechanical features correlated with clinical changes which were related to the foot, COP, ankle, and velocity. Finally, in a cohort of patients who had a change of 4 points in the iRODS, 37 biomechanical features correlated with the clinical change according to the same LME statistical test. Ten of these features were able to detect the clinical changes identified by both the iRODS and MRCss scales. These included spatiotemporal parameters (stride length and velocity) and angular features—four related to foot function, one to hip movement, and three to knee function.

Figure 9. Features that detected clinically significant changes in longitudinal analysis via the Wilcoxon model. The best and worst clinical assessments were selected in a cohort of patients who showed a difference of at least 2 points on the MRCss. Multiple comparisons were used, and a FDR-corrected p value < 0.05 was established to differentiate the features that significantly differed over the time. MRCss: Medical Research Council sum score.



- This study provided proof-of-concept that wearable technology effectively detects and grades gait impairment, captures clinically relevant changes, and could enhance gait assessment in routine care and clinical research for patients with peripheral neuropathies. These results were presented at the PNS Annual Meeting held in Copenhagen in June 2023 and in Montreal in June 2024. The manuscript reporting these findings was accepted for publication in the *Journal of NeuroEngineering and Rehabilitatio (Tejada-Illa C, Pegueroles J, Claramunt-Molet M, Pi-Cervera A, Heras-Delgado A, Gascón-Fontal J, Idelsohn-Zielonka S, Rico M, Vidal N, Martín-Aguilar L, Caballero-Ávila M, Lleixà C, Collet-Vidiella R, Llansó L, Carbayo Á, Vesperinas A, Querol L, Pascual-Goñi E. Digital biomechanical assessment of gait in patients with peripheral neuropathies. J Neuroeng Rehabil. 2025 Jul 13;22(1):159. doi: 10.1186/s12984-025-01694-w. PMID: 40653470; PMCID: PMC12257721.)*

- **We performed a second study to explore the potential of the wearable biomechanical technology to objectively detect balance impairments in a cohort of patients with inflammatory neuropathy.** We performed a transversal study analysing static features in patients with peripheral neuropathies using the Ephion Health System. Individuals wore the wearable system while performing the Romberg test with opened eyes and closed eyes. Patients selected for this analysis were classified according to their ataxia severity as previously described (Table 2). The Ellipse Method was employed to achieve

a comprehensive representation of balance and a LME model to assess the correlation between static features and items of MICARS-SARA scale. To evaluate balance impairment, an instability score was generated using the LASSO method.

- We included 45 CIDP patients, 27 IgM-MGUS- associated neuropathies, 9 MMN, 10 CMT and 117 healthy controls. Results for center of pressure (COP) and trunk movement according to the ataxia severity are displayed in Figure 10. Evaluations of both open-eye and closed-eye data during the Romberg test exhibit differences in COP and trunk movement according to ataxia severity. These differences were more evident when patients performed the test with their eyes closed specially in trunk range of movement. We then analyzed the correlation between the trunk and COP features extracted from inertial sensors with item 4 (corresponding to score when Romberg is performed with open eyes) and with item 5 (corresponding to score when Romberg is performed with closed eyes) of MICARS-SARA scale. The highest statistical significance in relation to the clinical scale was observed in the Romberg test performed with eyes closed. Additionally, the strongest correlations with the MICARS-SARA items were found in features derived from COP, particularly those related to the elliptical area. In contrast, during the Romberg test with eyes open, only minimal associations were observed across COP and trunk-related parameters with clinical scales. In order to objectively quantify balance impairment observed in both last analyses, an instability score was generated (Figure 11). Scores near 100 indicated control-like stability, while lower scores reflected greater variability and instability. Significant differences were found between control and pathological groups, obtaining scores significantly lower in patients' group. When we compared the different ataxia severity groups (Figure 4B), a significant reduction of the score was obtained when the ataxia severity increased. Significant differences were observed among the different severity groups, as well as between these groups compared to the control group.

  Figure 10. Descriptive analysis of COP and trunk movement during the Romberg test. (A) Romberg test performed with eyes opened and (B) with eyes closed. Patients were classified according to their ataxia severity. At the top of each figure, there are displayed the insoles which represent the ellipse centers as 'dots.' In grey, the area where the controls maintain the center of their ellipses and, in color, the subject's central position during the functional tests. The central graph represents the movement generated by the trunk during the test, enabling visualization of the trunk's position over time. At the bottom of each figure, the left and right graphs correspond to the ellipses from the insoles. The central graph corresponds to the ellipses from the trunk.

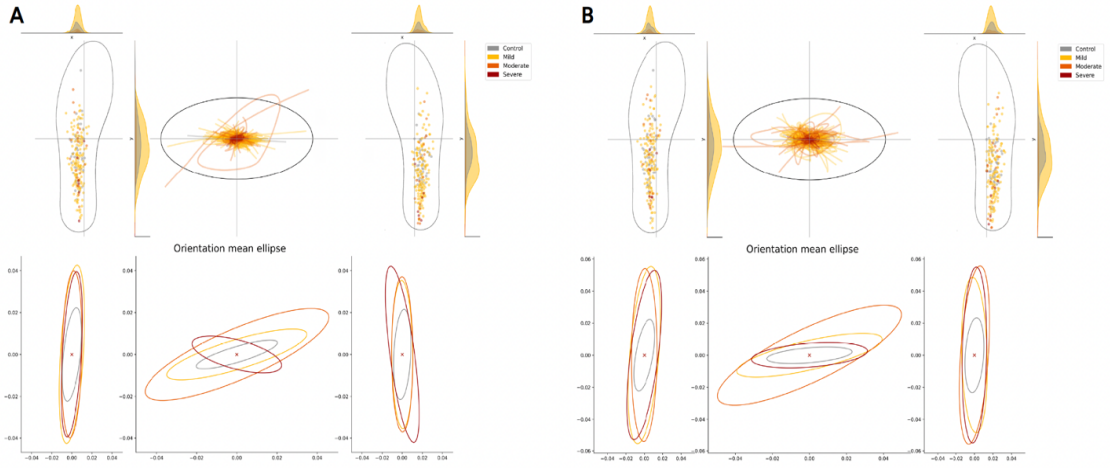
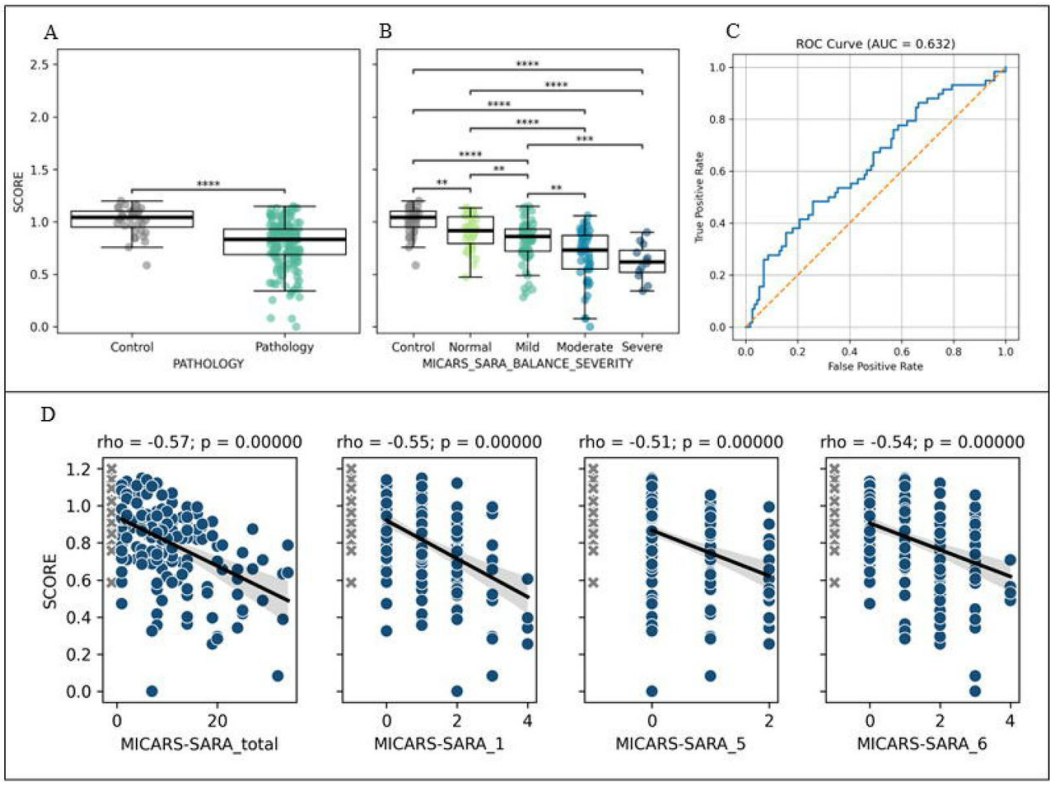


Figure 11. Digital Romberg's test



(A) Comparison of the normalized digital Romberg's test between healthy controls and patients with PN. (B) Comparison of the normalized digital Romberg's test across health controls and patient subgroups stratified by ataxia severity, demonstrating a progressive reduction in the score with increasing clinical severity. Boxes indicate median and interquartile range. Statistical significance is denoted as p< 0.05 (*) p < 0.01 (**), p < 0.001 (***). and p< 0.0001 (****). (C) Receiver operating characteristic (ROC) analysis of the score for discriminating patients with ataxia. The solid blue line represents the model performance while the dashed diagonal line indicates chance level. (D) Correlation of digital Romberg's test and items of: MICARS and SARA scale.

Scatter plots showing Spearman correlations between the instability score and MICARS and SARA total score and selected subitems (1, 5, and 6). With regression lines and 95% confidence intervals. PN: peripheral neuropathy: MICARS: Modified International Cooperative Ataxia Rating Scale: SARA Scale for the Assessment and Rating of Ataxia

- This study demonstrates that digital biomechanical assessment of stance is useful to quantify balance impairment in a large, heterogeneous cohort of patients with PN. Static balance features derived from inertial and plantar pressure sensors and integrated in an AI-generated digital Romberg's test captured alterations of static posture and correlated with clinical ataxia severity. The digital Romberg's test represents a promising, reproducible biomarker for both clinical trials, routine monitoring and treatment response assessment in patients with ataxia. This work is currently under peer review for publication and is publicly available as a preprint on *medRxiv (Tejada-Illa et al., Artificial intelligence-generated digital Romberg test for peripheral neuropathy monitoring, doi: https://doi.org/10.64898/2026.05.12.26353015).*

FUTURE DIRECTIONS:

1. NEW CIDP-SPECIFIC AUTOANTIBODIES: THIS STUDY FAILED TO DISCOVER NEW ANTIBODIES IN CIDP, AS CANDIDATE ANTIGENS IDENTIFIED BY INTEGRAL MOLECULAR MEMBRANE PROTEIN ARRAY WERE NOT VALIDATED BY IN HOUSE CBA AND ELISA. NOVEL ANTIBODY SCREENING STRATEGIES (ARRAYS, AND PHAGE IMMUNOPRECIPITATION ASSAYS) WILL BE APPLY IN THE FUTURE TO CONTINUE THE SEARCH FOR ANTIBODIES IN INFLAMMATORY NEUROPATHIES.

2. CIDP ACTIVITY BIOMARKERS: SERUM NEUROFILAMENT LIGHT CHAIN (SNFL) MAY SERVE AS A VALUABLE BIOMARKER FOR IDENTIFYING PATIENTS WITH ACTIVE DISEASE, PARTICULARLY WITHIN SPECIFIC SUBGROUPS OF INDIVIDUALS WITH INFLAMMATORY NEUROPATHIES. SNFL LEVELS WILL BE CORRELATED WITH NEUROLOGICAL EXAMINATION FINDINGS, CLINICAL ASSESSMENT SCALES, AND BIOMECHANICAL PARAMETERS OBTAINED THROUGH THE WEARABLE SYSTEM EMPLOYED IN SUBPROJECT 3.

3. WEARABLE BIOMECHANICAL TECHNOLOGY: WEARABLE BIOMECHANICAL TECHNOLOGY IS AN EFFECTIVE TOOL FOR OBJECTIVELY EVALUATING GAIT AND BALANCE IMPAIRMENT IN PATIENTS WITH INFLAMMATORY NEUROPATHIES. IT CAPTURES CLINICALLY RELEVANT CHANGES, AND COULD ENHANCE GAIT AND BALANCE ASSESSMENT IN ROUTINE CARE AND CLINICAL RESEARCH FOR PATIENTS WITH PERIPHERAL NEUROPATHIES. THE NEXT STEP WILL BE TO DEVELOP AN INTEGRATED COMPOSITE SCORE COMBINING STATIC AND DYNAMIC BIOMECHANICAL PARAMETERS, EVALUATE ITS CORRELATION WITH CLINICAL DISEASE STATUS, AND VALIDATE ITS PERFORMANCE IN INDEPENDENT EXTERNAL COHORTS.

APPENDIX:

During this period, the fellow also worked on additional research manuscripts in the field of autoimmune neuropathies, complementing the research supported by this grant.

1. *LLEIXÀ C, PASCUAL-GOÑI E, MARTÍN-AGUILAR L, CABALLERO-ÁVILA M, COLLET-VIDIELLA R, TEJADA-ILLA C, LLARCH P, GALLARDO E, BOERA-CARNICERO G, CALAHORRO V, CALLEGARI I, CORTESE A, DELMONT E, DEVAUX J, GIANNOTTA CC, NOBILE-ORAZIO E, HÖFTBERGER R, SELLNER J, HERDEWYN SAAJ, ALEJANDRA C, TORNÉ L, JERICÓ I, RINALDI S, SOMMER C, DOPPLER K, ARMANGUE T, TITULAER MJ, JACOBS BC, HUIZINGA R, WANSCHITZ JV, ORTIZ CASTELLON N, SPARASCI D, RIPELLINO P, PÉREZ-PÉREZ H, HORGA A,*

Alonso-Jiménez A, De Winter J, Jauregui A, de la Calle-Martin O, Martinez-Martinez L, Querol L. Specific HLA-DRB1 Alleles Associate With Anti-Caspr1 and Anti-CNTN1 Autoantibodies in Autoimmune Nodopathies. Neurol Neuroimmunol Neuroinflamm. 2026 Jul;13(4):e200602. doi: 10.1212/NXI.0000000000200602. Epub 2026 Jun 23. PMID: 42335443; PMCID: PMC13293632. **This multicenter study identified distinct HLA class II associations with anti-CNTN1 and anti-Caspr1 autoimmune nodopathies, supporting different genetic susceptibility profiles for these disease subtypes.**

2. *Caballero-Ávila M, Martín-Aguilar L, Pascual-Goñi E, Michael MR, Koel-Simmelink MJA, Höftberger R, Wanschitz J, Alonso-Jiménez A, Armangué T, Baars AE, Carbayo Á, Castek B, Collet-Vidiella R, De Winter J, Del Real MÁ, Delmont E, Diamanti L, Doneddu PE, Hiew FL, Gallardo E, Gonzalez A, Grinzinger S, Horga A, Iglseder S, Jacobs BC, Jauregui A, Killestein J, Pozza EL, Martínez-Martínez L, Nobile-Orazio E, Ortiz N, Pérez-Pérez H, Poppert KN, Ripellino P, Roche JC, Rodriguez de Rivera FJ, Rostasy K, Sparasci D, Tejada-Illa C, Teunissen CCE, Vegezzi E, Xuclà-Ferrarons T, Zach F, Wieske L, Eftimov F, Lleixà C, Querol L. Long-Term Follow Up in Anti-Contactin-1 Autoimmune Nodopathy. Ann Neurol. 2025 Mar;97(3):529-541. doi: 10.1002/ana.27142. Epub 2024 Nov 27. PMID: 39601182.* ***Research article that describes the long-term clinical course and biomarker profile of anti-CNTN1 autoimmune nodopathy, supporting the use of anti-CNTN1 antibodies, serum neurofilament light chain, and serum CNTN1 for disease monitoring.***

3. *Caballero-Ávila M, Pascual-Goñi E, Lleixà C, Martín-Aguilar L, Collet-Vidiella R, Querol L. The changing landscape of primary autoimmune neuropathies. Nat Rev Neurol. 2025 Oct;21(10):544-555. doi: 10.1038/s41582-025-01133-3. Epub 2025 Sep 5. PMID: 40913126.* **Review of recent advances in autoimmune neuropathies, including disease mechanisms, novel biomarkers, updated diagnostic criteria, and emerging targeted therapies.**

4. *Pascual-Goñi E, Caballero-Ávila M, Querol L. Antibodies in Autoimmune Neuropathies: What to Test, How to Test, Why to Test. Neurology. 2024 Aug 27;103(4):e209725. doi: 10.1212/WNL.0000000000209725. Epub 2024 Aug 1. Erratum in: Neurology. 2025 Feb 11;104(3):e210298. doi: 10.1212/WNL.0000000000210298. PMID: 39088795; PMCID: PMC11319070.* **Review of the clinical utility of autoantibodies in the diagnosis and management of autoimmune neuropathies, with a focus on autoimmune nodopathies and their implications for diagnosis and treatment.**

5. *Caballero-Ávila M, Martin-Aguilar L, Collet-Vidiella R, Querol L, Pascual-Goñi E. A pathophysiological and mechanistic review of chronic inflammatory demyelinating polyradiculoneuropathy therapy. Front Immunol. 2025 Apr 14;16:1575464. doi: 10.3389/fimmu.2025.1575464. PMID: 40297573; PMCID: PMC12034639.* **Review of current concepts in CIDP pathophysiology and emerging targeted therapies, with a focus on complement inhibition and FcRn blockade.**

6. *Elba Pascual-Goñi, Paula Llarch , Anaís Mariscal, Eugenia Martínez-Hernandez , Solange Kapetanovic , Young Gi Min , Lorena Martín-Aguilar, Esther Moga, Tania Mederer, Gemma Riesco-Navarro, Gemma Olivé-Cirera, Cinta Lleixà, Clara Tejada Illa, Marta Caballero-Ávila, Roger Collet-Vidiella, Juan Castilla-Silgado, Ana Beatriz Serafim, Laura Naranjo, Raquel Ruiz-García, Jung-Joon Sung, Ricard Rojas, Jordi Lopez-Pardo, Eduard Gallardo, Lidia Sabater, Luis Querol. Anti-HNK-1 IgM and serum neurofilament light chain for diagnosis and disease monitoring in anti-MAG neuropathy (Under Review)* **A research article that describes a novel live anti-HNK-1 cell-based assay for the diagnosis of anti-MAG neuropathy and highlights the complementary role of anti-HNK-1 antibodies and serum neurofilament light chain in disease monitoring.**